Dalton Transactions

Accepted Manuscript

ROYAL SOCIETY OF CHEMISTRY

www.rsc.org/dalton

Journal Name
ARTICLE
Cite this: DOI: 10.1039/x0xx00000x
Received 00th January 2012,
Accepted 00th January 2012
DOI: 10.1039/x0xx00000x
www.rsc.org/

RSCPublishing

Trinuclear Alkyl Hydrido Rare-Earth Complexes Supported by Amidopyridinato Ligands: Synthesis, Structures, C−Si Bond Activation and Catalytic Activity in Ethylene Polymerization

Dmitry M. Lyubov,[a,c] Anton V. Cherkasov,[a,c] Georgy K. Fukin,[a,c] Sergey Yu. Ketkov,[a,c] Andrey S. Shavyrin[a] and Alexander A. Trifonov[a,b,c]*

The reaction of $Ap^{9Me}Lu(CH_2SiMe_3)_2(thf)$ (Ap^{9Me} = (2,4,6-trimethylphenyl)[6-(2,4,6-triisopropylphenyl)pyridine-2-yl]amido ligand) with two molar equivalents of $PhSiH_3$ affords a trinuclear alkyl-hydrido cluster $[(Ap^{9Me}Lu)_3(\mu^2\text{-}H)_3(\mu^3\text{-}H)_2(CH_2SiMe_3)(thf)_2]$. The analogous reactions with $Ap^{9Me}Ln(CH_2SiMe_3)_2(thf)$ (Ln = Y, Yb) are more complex and result in the formation of mixtures of two types of trinuclear alkyl-hydrido complexes $[(Ap^{9Me}Ln)_3(\mu^2\text{-}H)_3(\mu^3\text{-}H)_2(CH_2SiMe_3)(thf)_2]$ and $[(Ap^{9Me}Ln)_3(\mu^2\text{-}H)_3(\mu^3\text{-}H)_2(CH_2SiH_2Ph)(thf)_2]$ differing in the alkyl group. The DFT calculations of $[(Ap^*Y)_3(\mu^2\text{-}H)_3(\mu^3\text{-}H)_2(CH_2SiMe_3)(thf)_2]$ (Ap* = (2,6-diisopropylphenyl)[6-(2,4,6-triisopropylphenyl) pyridine-2-yl]amido ligand) confirm localization of the HOMO on the Ap*−Y(1A)−CH_2SiMe_3 fragment thus explaining its enhanced reactivity. Analysis of the electron density distribution reveals the Y−H and H−H bonding interactions in the $(Y)_3(\mu^2\text{-}H)_3(\mu^3\text{-}H)_2$ moiety. The NMR studies of diamagnetic complexes $[(Ap^{9Me}Lu)_3(\mu^2\text{-}H)_3(\mu^3\text{-}H)_2(CH_2SiMe_3)(thf)_2]$ and $[(Ap^*Y)_3(\mu^2\text{-}H)_3(\mu^3\text{-}H)_2(CH_2SiMe_3)(thf)_2]$ demonstrated that the trinuclear cores are retained in the solution and revealed exchange between μ^3- and μ^2-bridging hydrido ligands. Complexes $[(Ap^*Ln)_3(\mu^2\text{-}H)_3(\mu^3\text{-}H)_2(CH_2SiMe_3)(thf)_2]$, cationic yttrium hydrido cluster $[(Ap^*Y)_3(\mu^2\text{-}H)_3(\mu^3\text{-}H)_2(thf)_3]^+[B(C_6F_5)_4]^-$ as well as $[(Ap^{9Me}Ln)_3(\mu^2\text{-}H)_3(\mu^3\text{-}H)_2(CH_2SiMe_3)(thf)_2]$ proved to be active in catalysis of ethylene polymerization under mild conditions.

Introduction

Despite the fact that rare-earth hydrides are known for over thirty years[1] they remain in the focus of attention because of their unique reactivity[2] and high activity in a variety of catalytic transformations.[3] Until recently rare-earth metal hydrides were represented exclusively by sandwich and halfsandwich-type ("constrained geometry")[1d,4] monohydrido complexes which adopt dimeric structures due to μ-hydrido ligands bridging two metal centers. Application of bulky cyclopentadienyl ligands allowed for stabilization of terminal hydrido species[2,5] which demonstrated exceptionally high reactivity. The synthesis of monomeric hydrides presents one of the challenges of the modern organorare-earth chemistry. During the past decade some progress has been done in the field of the synthesis of hydrido species supported by non-cyclopentadienyl ligands nevertheless these compounds still remain scarce.[6] The first polyhydrido clusters assembled from dihydrido $[CpLnH_2]$ building blocks containing substituted cyclopentadienyl ligands were reported in 2001, and their stoichiometric and catalytic chemistry was developed by Hou and co-workers.[7] The synthesis of rare-earth polyhydrido clusters of various nuclearity proved to be feasible due to application of non-cyclopentadienyl coordination environments.[8] Hydrido complexes of divalent lanthanides also remain poorly explored: just three of them are known to date.[9]

Recently we reported on the synthesis, molecular structures, reactivity and catalytic activity in ethylene polymerization of a family of trinuclear rare-earth metal alkyl-hydrido and cationic hydrido clusters supported by sterically demanding (2,6-diisopropylphenyl)[6-(2,4,6-triisopropylphenyl)pyridine-2-yl] amido ligand (Ap*H) $[(Ap^*Ln)_3(\mu^2\text{-}H)_3(\mu^3\text{-}H)_2(CH_2SiMe_3)(thf)_2]$ (Ln = Y, Er, Yb, Lu).[10] Herein we describe the synthesis and the structures of new trinuclear rare-earth alkyl hydrido clusters stabilized by less bulky (2,4,6-trimethylphenyl)[6-(2,4,6-triisopropylphenyl)pyridine-2-yl]amido ligand ($Ap^{9Me}H$).[11]

Results and Discussions

For the synthesis of bis(alkyl) rare-earth complexes supported by (2,4,6-trimethylphenyl)[6-(2,4,6-triisopropylphenyl)pyridine -2-yl]amido (Ap^{9Me}) ligand the alkane elimination approach was employed. The NMR-scale reactions (1:1 molar ratio, d^6-benzene, 20 °C) were carried out for diamagnetic Y and Lu and evidenced clear and quantitative formation of amidopyridinato bis(alkyl) complexes and release of $SiMe_4$. The NMR-tube reactions of $Ln(CH_2SiMe_3)_3(thf)_2$ (Ln = Y, Lu) with two molar equivalents of $Ap^{9Me}H$ (d^6-benzene, 20 °C) revealed that only one equivalent is involved into the reaction, while the second one remains unreacted. The reactions stop at the stage of formation of amidopyridinato bis(alkyl) species obviously due to the steric constraint within the coordination sphere of rare-earth metal which hampers coordination of the second $Ap^{9Me}H$ ligand.

The preparative-scale reactions of $Ln(CH_2SiMe_3)_3(thf)_2$ (Ln = Y,[12a] Yb,[12b] Lu[12b]) with equimolar amounts of $Ap^{9Me}H$ were carried out at 0 °C in hexane and afforded bis(alkyl) derivatives $Ap^{9Me}Ln(CH_2SiMe_3)_2(thf)$ (Ln = Y (**1Y**),[11] Yb (**1Yb**), Lu (**1Lu**)) (Scheme 1).

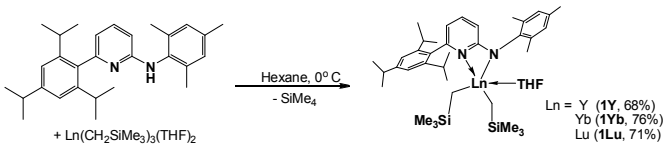

Scheme 1.

The in situ synthesis of complex **1Y** and its characterization by ^1H and ^{13}C NMR spectroscopy was previously reported.[11] Bis(alkyl) complexes **1Ln** were isolated as pale yellow (**1Y**, **1Lu**) or dark red (**1Yb**) microcrystalline solids in reasonable yields. Unfortunately all our attempts to obtain monocrystalline samples of **1Ln** suitable for X-Ray structure determination failed, nevertheless the compounds are unambiguously authenticated by the means of spectroscopic methods and microanalysis. In the ^1H NMR spectrum of **1Lu** the methylene protons of alkyl group attached to the metal atom appear as a sharp singlet at 0.65 ppm, in the $^{13}C\{^1H\}$ spectrum the appropriate carbons give rise to a singlet at 46.1 ppm. Thermostabilities of diamagnetic bis(alkyl) complexes **1Y** and **1Lu** were evaluated by ^1H NMR spectroscopy (d^6-benzene solution, 20 °C). The complexes turned out to be rather stable under these conditions: in one week for **1Y** decomposition was ~30% and for **1Lu** ~20% respectively. Decompositions of **1Y** and **1Lu** occur with $SiMe_4$ elimination. Previously we reported several examples of thermal decomposition of rare earth metal alkyl complexes supported by amidopyridinato ligands resulting in intramolecular activation of sp^3 and sp^2 C-H bonds,[13] however for **1Y** and **1Lu** no evidences of C-H bond activation of Ap^{9Me} ligand was detected.

Bis(alkyl) species **1Ln** were used as precursors for the synthesis of the related dihydrido derivatives. The σ-bond metathesis reaction of **1Ln** with two equivalents of $PhSiH_3$ was carried out in hexane at room temperature. It was found that the reaction of **1Lu** similarly to the previously reported reactions of Ap^*H[10] affords a trinuclear alkyl-hydrido cluster

$[(Ap^{9Me}Lu)_3(\mu^2\text{-}H)_3(\mu^3\text{-}H)_2(CH_2SiMe_3)(thf)_2]$ (**2Lu**)

(Scheme 2). In order to replace the remaining alkyl group by hydrido ligand a ten-fold molar excess of $PhSiH_3$ was used and the reaction time was increased to 24 h. Nevertheless complex **2Lu** was the sole lutetium containing product isolated from the reaction mixture (60% yield). Application of H_2 (hexane, 3 bar, 36 h) did not allow to replace the alkyl group neither; **2Lu** was isolated in 62% yield. Complex **2Lu** is extremely air- and moisture-sensitive crystalline solid; it is highly soluble in hexane and pentane. Complex **2Lu** can be kept in solid state or in d^6-benzene solutions under dry argon or in sealed evacuated tubes at 20 °C for several weeks without decomposition.

The X-ray study of monocrystalline samples of **2Lu** was carried out and established the overall geometry of the molecule and the order of connectivity of the atoms. However, the poor quality of the experiment does not allow for the discussion of the bond distances and angles of **2Lu**. Complex **2Lu** adopts a trinuclear structure similar to those formerly detected for the related alkyl-hydrido complexes $[(Ap^*Ln)_3(\mu^2\text{-}H)_3(\mu^3\text{-}H)_2(CH_2SiMe_3)(thf)_2]$ (Ln = Y, Er, Yb, Lu).[10] The molecular structure of **2Lu** is depicted in Fig. 1. Complex **2Lu** is composed by three $Ap^{9Me}Lu$ fragments, one of the lutetium ions maintains one CH_2SiMe_3 group, while two others are coordinated by one THF molecule.

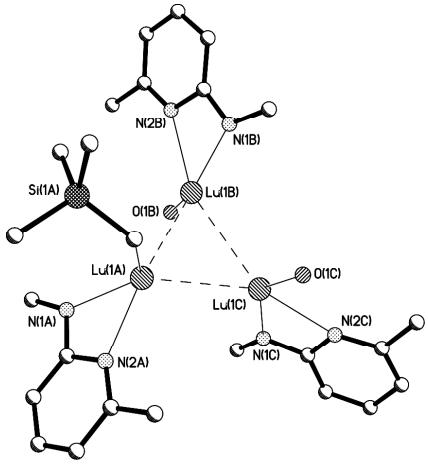

Fig. 1. Molecular structure of complex **2Lu**; the 2,4,6-$iPr_3C_6H_2$, 2,4,6-$Me_3C_6H_2$ substituents in the Ap^{9Me} ligands and methylene groups of THF molecules are omitted for clarity.

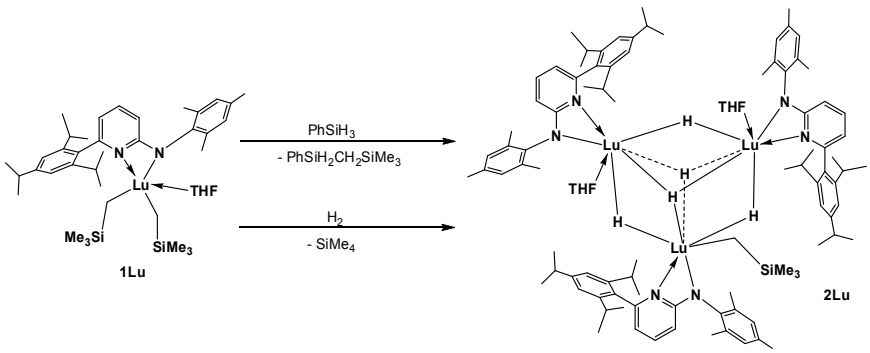

Scheme 2.

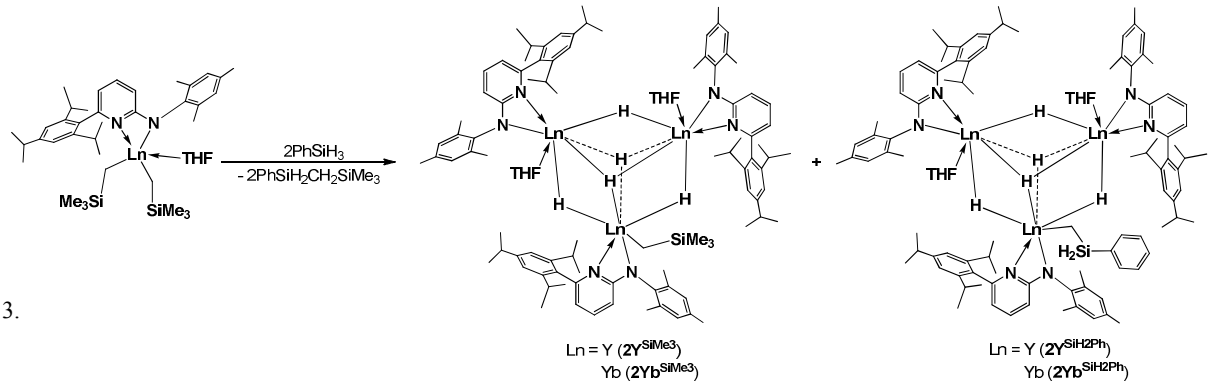

Scheme 3.

The similar synthetic procedure was applied for the synthesis of alkyl-hydrido species of yttrium and ytterbium. The reactions of **1Y** and **1Yb** with $PhSiH_3$ were carried out under analogous conditions (1:2 molar ratio, hexane, 20 °C) however unlike the reaction of **1Lu** and the previously reported reactions of $Ap^*Ln(CH_2SiMe_3)_2(thf)$ (Ln = Y, Er, Yb, Lu)[10] the mixtures of two co-crystallizing trinuclear clusters $\mathbf{2Ln^{SiMe3}}$ and $\mathbf{2Ln^{SiH2Ph}}$ (Scheme 3) were isolated. The only difference between clusters $\mathbf{2Ln^{SiMe3}}$ and $\mathbf{2Ln^{SiH2Ph}}$ is the alkyl group covalently bonded to the rare-earth metal. Thus complexes $\mathbf{2Ln^{SiMe3}}$ contain CH_2SiMe_3 groups which originate from the parent complexes **1Ln** while the $\mathbf{2Ln^{SiH2Ph}}$ are furnished with CH_2SiH_2Ph fragments. According to the X-Ray diffraction studies the reaction of **1Y** with $PhSiH_3$ results in the formation of 2:1 mixture of complexes $\mathbf{2Y^{SiMe3}}$ and $\mathbf{2Y^{SiH2Ph}}$, while in the case of $\mathbf{2YbSiMe3}$ and $\mathbf{2YbSiH2Ph}$ both products are presented in the mixture in equivalent amounts. Complexes $\mathbf{2Ln^{SiMe3}}$ and $\mathbf{2Ln^{SiH2Ph}}$ cannot be separated by crystallization due to their similar solubilities in organic solvents.

It should be noted, that the result of the reaction of **1Yb** with $PhSiH_3$ is reproducible and complex $\mathbf{2Yb^{SiMe3}/Yb^{SiH2Ph}}$ can be isolated after crystallization from solution in hexane in reasonable yield 68%, while complex $\mathbf{2Y^{SiMe3}/Y^{SiH2Ph}}$ was isolated in 7% yield and all our attempts to reproduce the synthesis failed. Unfortunately no satisfactory NMR and microanalysis data were obtained for $\mathbf{2Y^{SiMe3}/Y^{SiH2Ph}}$. The NMR-tube reaction of **1Y** with two molar equivalents of $PhSiH_3$ was carried out in d^6-benzene solution at ambient temperature. The ^1H and $^{13}C\{^1H\}$ spectra of the reaction mixture in ~20 min indicated quantitative formation of the reaction by-product $PhSiH_2CH_2SiMe_3$, however rapid disappearance of the species containing Y−alkyl and Y−H fragments was noticed. Insufficient bulkiness of the Ap^{9Me} ligand is the most probable reason of instability of alkyl-hydrido species of yttrium having comparatively large ion.

The formation of $LnCH_2SiH_2Ph$ moiety can be rationalized either by abnormal path of the σ-bond metathesis step (Scheme 4, A) or by C−Si bond activation of the reaction product $PhSiH_2CH_2SiMe_3$ at $LnCH_2SiMe_3$ site (Scheme 4, B). As evidenced by the detection of $HSiMe_3$ in the volatile reaction products of **1Yb** with $PhSiH_3$ by GC-MS (see ESI Fig. SI5) the path A is responsible for the formation of $LnCH_2SiH_2Ph$ fragment. $Me_3SiCH_2SiMe_3$ was not detected in the reaction mixture by GC-MS and by ^1H NMR.

According to the X-Ray analysis complexes $\mathbf{2Ln^{SiMe3}/Ln^{SiH2Ph}}$ crystallize in triclinic space group *P*-1 with two molecules in the unit sell. Molecular structures of $\mathbf{2Ln^{SiMe3}/Ln^{SiH2Ph}}$ are depicted in Fig. 2; the crystal and structural refinement data for $\mathbf{2Ln^{SiMe3}/Ln^{SiH2Ph}}$ are summarized in Table 1.

Similarly to the previously reported Ap*-containing alkyl hydrido clusters the Ln−N bonds in $\mathbf{2Ln^{SiMe3}/Ln^{SiH2Ph}}$ are not equivalent: one Ln−N bond is covalent ($Ln-N_{amido}$ 2.296(6)–2.325(6) Å for $\mathbf{2Y^{SiMe3}/Y^{SiH2Ph}}$; 2.241(6)–2.297(7) Å for $\mathbf{2YbSiMe3/YbSiH2Ph}$) while the second one is coordination bond ($Ln-N_{pyr}$ 2.490(6)–2.526(6) Å for $\mathbf{2Y^{SiMe3}/Y^{SiH2Ph}}$; 2.454(6)–2.501(6) Å for $\mathbf{2YbSiMe3/YbSiH2Ph}$). The Y−C distances in $\mathbf{2Y^{SiMe3}/Y^{SiH2Ph}}$ are similar – 2.446(6) Å, while in $\mathbf{2YbSiMe3/YbSiH2Ph}$ the bond between Yb and methylene carbon of CH_2SiMe_3 group (2.341(4) Å) is slightly longer than that to carbon atom of CH_2SiH_2Ph fragment (2.301(4) Å). Short contact between yttrium atom and silicon atom of CH_2SiH_2Ph ligand (Y(1A)−Si(1') 3.226(5)Å) and strongly distorted geometry around the sp^3-hybridized carbon atom (Si(1')−C(30A)−Y(1A) 97.4(3)°) are indicative of an agnostic interaction. However no agostic interaction was detected in the ytterbium compounds. The absence of agostic interaction in ytterbium alkyl-hydrido clusters $\mathbf{2YbSiMe3/YbSiH2Ph}$ obviously is associated with smaller ionic radius of the Yb^{3+} compared to Y^{3+} ($R(Y^{3+})$ = 0.960 Å; $R(Yb^{3+})$ = 0.925 Å).[14] The shorter Ln−Ln (compare: for Yb 3.3492(5)–3.4227(6) Å for Y 3.456(1)–3.508(1) Å) and Ln−N distances in the case of $\mathbf{2YbSiMe3/YbSiH2Ph}$ prevent Yb−Si agostic interactions.

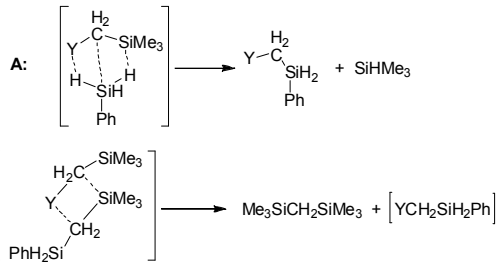

Scheme 4.

Journal Name
ARTICLE
RSCPublishing

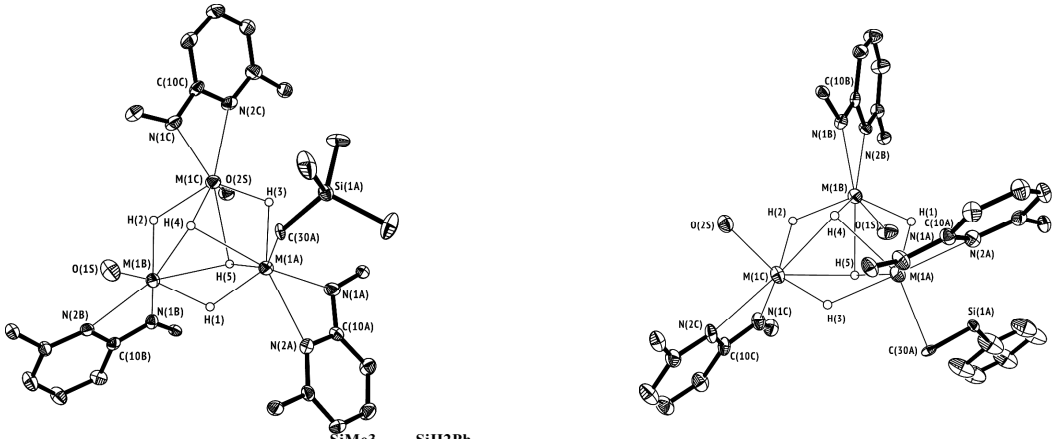

Fig. 2. Molecular structure of complexes **2Ln^{SiMe3}/Ln^{SiH2Ph}** with 30% probability ellipsoids; the *i*Pr, Me substituents in the Ap^{9Me} ligands and methylene groups of THF molecules are omitted for clarity. Selected distances [Å] and angles [°] for **2Y^{SiMe3}/Y^{SiH2Ph}**: Y(1A)−Y(1B) 3.500(1), Y(1A)−Y(1C) 3.506(1), Y(1B)−Y(1C) 3.455(1), Y(1A)−N(1A) 2.318(5), Y(1A)−N(2A) 2.508(5), Y(1A)−C(30A) 2.454(5), Y(1A)−Si(1A^{Ph}) 3.226(5), Y(1A)−H(1) 2.03(2), Y(1A)−H(3) 2.15(2), Y(1A)−H(4) 2.22(2), Y(1A)−H(5) 2.27(2), Y(1B)−N(1B) 2.298(5), Y(1B)−N(2B) 2.528(5), Y(1B)−O(1S) 2.322(4), Y(1B)−H(1) 2.09(2), Y(1B)−H(2) 2.12(2), Y(1B)−H(4) 2.25(2), Y(1B)−H(5) 2.30(2), Y(1C)−N(1C) 2.301(5), Y(1C)−N(2C) 2.492(5), Y(1C)−O(2S) 2.346(4), Y(1C)−H(2) 2.09(2), Y(1C)−H(3) 2.06(2), Y(1C)−H(4) 2.22(2), Y(1C)−H(5) 2.23(2); N(1A)−Y(1A)−N(2A) 55.6(2), Y(1B)−Y(1A)−Y(1C) 59.11(2), N(1B)−Y(1B)−N(2B) 56.1(2), Y(1C)−Y(1B)−Y(1A) 60.56(2), N(1C)−Y(1C)−N(2C) 56.3(2), Y(1B)−Y(1C)−Y(1A) 60.33(2). Selected distances [Å] and angles [°] for **2Yb^{SiMe3}/Yb^{SiH2Ph}**: Yb(1A)−Yb(1B) 3.4078(5), Yb(1A)−Yb(1C) 3.4227(6), Yb(1B)−Yb(1C) 3.3492(5), Yb(1A)−N(1A) 2.297(7), Yb(1A)−N(2A) 2.494(6), Yb(1A)−C(10A) 2.853(7), Yb(1A)−C(30A^{SiPh}) 2.301(4), Yb(1A)−C(30A^{SiMe3}) 2.34(1), Yb(1A)−Si(1A^{Ph}) 3.421(5), Yb(1A)−H(1) 2.05(2), Yb(1A)−H(3) 2.05(2), Yb(1A)−H(4) 2.22(2), Yb(1A)−H(5) 2.22(2), Yb(1B)−N(1B) 2.241(6), Yb(1B)−N(2B) 2.501(6), Yb(1B)−C(10B) 2.820(8), Yb(1B)−O(1S) 2.278(6), Yb(1B)−H(1) 2.05(2), Yb(1B)−H(2) 2.05(2), Yb(1B)−H(4) 2.22(2), Yb(1B)−H(5) 2.22(2), Yb(1C)−N(1C) 2.258(6), Yb(1C)−N(2C) 2.454(6), Yb(1C)−C(10C) 2.820(7), Yb(1C)−O(2S) 2.281(6), Yb(1C)−H(2) 2.05(2), Yb(1C)−H(3) 2.052(2), Yb(1C)−H(4) 2.22(2), Yb(1C)−H(5) 2.22(2); Yb(1B)−Yb(1A)−Yb(1C) 58.72(1), Yb(1C)−Yb(1B)−Yb(1A) 60.86(1), Yb(1B)−Yb(1C)−Yb(1A) 60.42(1), N(1A)−Yb(1A)−N(2A) 56.2(2), N(1B)−Yb(1B)−N(2B) 56.7(2), N(1C)−Yb(1C)−N(1C) 56.8(2).

Table 1. Crystallographic data and structure refinement details for **2Y^{SiMe3}/Y^{SiH2Ph}** and **2Yb^{SiMe3}/Yb^{SiH2Ph}**.

	2Y^{SiMe3}/Y^{SiH2Ph}	2Yb^{SiMe3}/Yb^{SiH2Ph}
Empirical formula	$C_{118}H_{184.34}N_6O_2SiY_3$	$C_{105.75}H_{156.50}N_6O_2SiYb_3$
Formula weight	2013.87	2091.08
Temperature [K]	100(2)	150(2)
Wavelength [Å]	0.71073	0.71073
Crystal system, space group	Triclinic, *P-1*	
a [Å]	16.2230(9)	16.471(1)
b [Å]	17.7813(9)	17.640(2)
c [Å]	20.820(1)	19.774(2)
α [°]	75.647(1)	88.406(2)
β [°]	84.259(1)	76.212(2)
γ [°]	85.635(1)	84.783(2)
V [Å^3]	5781.1(5)	5556.1(8)
Z, D_c [g m^{-3}]	2, 1.157	2, 1.250
Absorption coefficient [mm^{-1}]	1.552	2.560
F(000)	2163	2146
Crystal size [mm]	0.45 × 0.40 × 0.21	0.21 × 0.20 × 0.12
Θ Range for data collection [°]	1.75 – 24.13	1.58 – 26.00
Completeness to Θ, %	98.6	99.0
Limiting indices	$-18 \le h \le 18$ $-20 \le k \le 20$ $-23 \le l \le 23$	$-20 \le h \le 16$ $-21 \le k \le 21$ $-24 \le l \le 22$
Reflections collected / unique (R_{int})	40315 / 18151 (0.0944)	33185 / 21618 (0.0547)
GOF on F^2	0.941	1.032
Data / restraints / parameters	18151 / 118 / 949	21618 / 149 / 1112
Final *R* indices [I>2σ(*I*)]	*R*1 = 0.0887, w*R*2 = 0.2136	*R*1 = 0.0796, w*R*2 = 0.1876
R indices (all data)	*R*1 = 0.1802, w*R*2 = 0.2515	*R*1 = 0.1495, w*R*2 = 0.2102
Largest diff. peak and hole [e Å^{-3}]	1.792 and −1.137	3.713 and −2.004

Journal Name
ARTICLE
RSCPublishing

DFT calculations

In order to get a deeper insight into the factors driving assembling of trinuclear alkyl-hydrido clusters their electronic structures were studied at the PBEPBE/DGDZVP level of DFT using $(Ap^*Y)_3(\mu^2\text{-}H)_3(\mu^3\text{-}H)_2(CH_2SiMe_3)(thf)_2$ (**3Y**) as a model compound without simplifications of the molecular structure. The **3Y** HOMO energy (−4.20 eV) appears to be very close to that calculated in our previous work[10b] for the simplified molecule containing unsubstituted Ap ligands and a methyl group instead of CH_2SiMe_3 (−4.24 eV). The HOMO is localized on the Ap*−Y(1A)−CH_2SiMe_3 fragment (Fig. 3). This confirms our earlier conclusions on the high reactivity of the metal-alkyl bond and the possibility of the formation of a stable cationic cluster after detachment of the alkyl group and an electron.[10b] To investigate intramolecular interactions in the $Y_3(\mu^2\text{-}H)_3(\mu^3\text{-}H)_2$ system we analyzed the topology of the electron density and reduced electron density gradient (RDG).[15] The dimensionless RDG function $s = |\nabla\boldsymbol{\rho}|/(2(3\pi^2)^{1/3}\boldsymbol{\rho}^{4/3})$, where $\boldsymbol{\rho}$ is the electron density, is useful in revealing weak noncovalent bonds. Attractive interactions can then be identified by the negative sign of the λ_2 eigenvalue of the electron-density Hessian matrix.[15c]

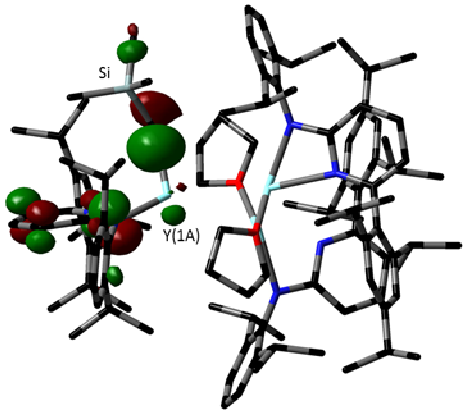

Fig. 3. $(Ap^*Y)_3(\mu^2\text{-}H)_3(\mu^3\text{-}H)_2(CH_2SiMe_3)(thf)_2$ (**3Y**) HOMO isosurface (isovalue 0.05 a.u.).

The electron density distribution demonstrates clearly the symmetry distortion in the $Y_3(\mu^2\text{-}H)_3$ fragment which arises from nonequivalence of the Y(1A) atom bearing the alkyl group (Fig. 4). An area of decreased electron density is formed near the line connecting the H(1) and H(3) atoms bonded to Y(1A). The $\boldsymbol{\rho}$ values in the Y−H bonding critical points (Table 2, Fig. 4) show that the Y(1A)−H bonds are weaker than Y(1B)−H and Y(1C)−H. The weakest interactions are observed for the axial H(4) and H(5) atoms.

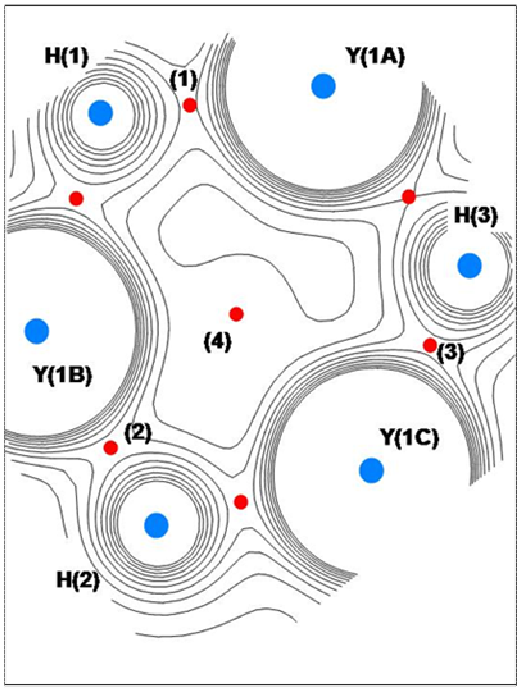

Fig. 4. Electron density contour maps (0.01–0.10 a.u. range, step 0.01 a.u.) in the Y(1A)Y(1B)Y(1C) plane of $(Ap^*Y)_3(\mu^2\text{-}H)_3(\mu^3\text{-}H)_2(CH_2SiMe_3)(thf)_2$ (**3Y**). (3,−1) Critical points (1)−(3) characterise the Y(1A)−H, Y(1B)−H and Y(1C)−H bonds, respectively. The (4) bonding critical point corresponds to the H(4)−H(5) interaction.

The $(Y)_3(\mu^2\text{-}H)_3(\mu^3\text{-}H)_2$ contribution to the RDG function (Fig. 5) reveals bonding Y−H interactions. Interestingly, the λ_2 eigenvalues show that there are also weak attractive H−H interactions. This can be a result of overlap of the hydride anion wavefunctions resulting in electron density delocalization within the $(Y)_3(\mu^2\text{-}H)_3(\mu^3\text{-}H)_2$ fragment. An evidence of such a delocalization is seen e.g. in the contour map of HOMO-4 (see ESI, Fig. SI10). Accordingly, the electron density topology analysis reveals a H(4)−H(5) (3,−1) critical point. The corresponding $\boldsymbol{\rho}$ value (0.019 a.u.) is close to those characterizing the Y(1A)−H(4) and Y(1A)−H(5) bonds (Table 2).

Table 2. Calculated Y−H interatomic distances d (Å) and the electron density ρ (a.u.) in the Y−H bonding critical points of $(Ap^*Y)_3(\mu^2\text{-}H)_3(\mu^3\text{-}H)_2(CH_2SiMe_3)(thf)_2$ (**3Y**).

Bond	d	ρ	Bond	d	ρ	Bond	d	ρ
Y(1A)-H(1)	2.19	0.040	Y(1B)-H(1)	2.14	0.045	Y(1C)-H(1)	2.12	0.047
Y(1A)-H(3)	2.19	0.040	Y(1B)-H(2)	2.13	0.047	Y(1C)-H(3)	2.15	0.044
Y(1A)-H(4)	2.52	0.021	Y(1B)-H(4)	2.24	0.037	Y(1C)-H(4)	2.28	0.034
Y(1A)-H(5)	2.42	0.025	Y(1B)-H(5)	2.26	0.036	Y(1C)-H(5)	2.23	0.037

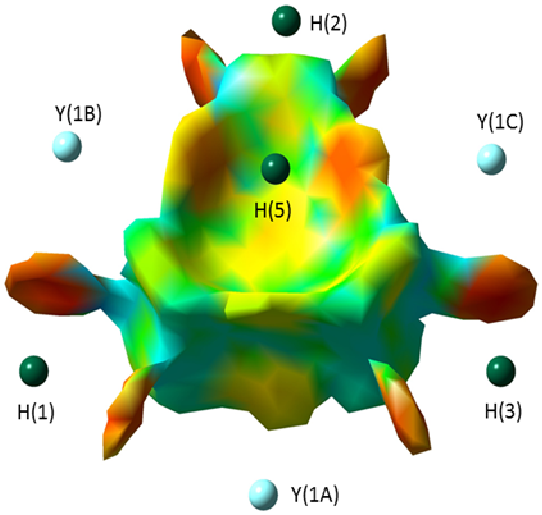

Fig. 5. Reduced density gradient isosurface (s = 0.5) for the $(Y)_3(\mu^2\text{-}H)_3(\mu^3\text{-}H)_2$ fragment of $(Ap^*Y)_3(\mu^2\text{-}H)_3(\mu^3\text{-}H)_2(CH_2SiMe_3)(thf)_2$. The s isosurfaces are colored on a red-yellow-green-blue scale according to the λ_2 eigenvalues of the electron density hessian, ranging from −0.05 to 0.05 a.u. Red indicates attractive interactions, and blue indicates nonbonded overlap

Table 3. Calculated Mulliken/NBO atomic charges for selected atoms in $(Ap^*Y)_3(\mu^2\text{-}H)_3(\mu^3\text{-}H)_2(CH_2SiMe_3)(thf)_2$ (**3Y**).

Atom	Charge	Atom	Charge	Atom	Charge
Y(1A)	0.92/1.61	Y(1B)	0.89/1.57	Y(1C)	0.85/1.57
N(1A)	-0.62/-0.83	N(1B)	-0.63/-0.83	N(1C)	-0.64/-0.83
N(2A)	-0.40/-0.65	N(2B)	-0.40/-0.66	N(2C)	-0.41/-0.66
C(30A)	-1.09/-1.54	H(1)	-0.24/-0.51	H(2)	-0.21/-0.49
H(3)	-0.24/-0.51	H(4)	-0.19/-0.48	H(5)	-0.18/-0.47

The charge distribution (Table 3) shows that Y(1A) bearing the alkyl group is slightly more positive than two other Y atoms. The N(1) charge is substantially more negative as compared to N(2). This suggests more ionic character of the $Y-N_{amido}$ interaction which agrees with the longer $Y-N_{amido}$ distances. The charge of H(2) located between Y(1B) and Y(1C) is less negative than that of the H(1) and H(3) atoms interacting with the more positive Y(1A). μ^3-Atoms H(4) and H(5) are less negatively charged than H(2).

NMR Investigation of Trinuclear Alkyl-Hydrido Clusters

To ascertain that the trinuclear structures are retained in solution and to elucidate the effect of Ap ligands on the solution behavior of the trinuclear alkyl-hydrido clusters the ^1H and $^{13}C\{^1H\}$ NMR spectra of **2Lu** and of the previously reported complexes $[(Ap^*Ln)_3(\mu^2\text{-}H)_3(\mu^3\text{-}H)_2(CH_2SiMe_3)(thf)_2]$ (Ln = Y (**3Y**), Lu (**3Lu**))[10] were investigated in details. According to the ^1H NMR spectra alkyl-hydrido complexes **2Lu** and **3Y**, **3Lu** retain their trinuclear structures in d^6-benzene and d^8-THF solutions. Most of the $^{13}C\{^1H\}$ and some of the ^1H NMR signals attributed to the amidopyridinate ligands are observed as sets of three signals in 1:1:1 ratio (if not overlapped). This is caused by nonequivalence of three Ap ligands in these complexes. Moreover, there are three signals in the $^{89}Y\{^1H\}$ NMR spectrum of **3Y** also indicating dissymmetry of this complex. It has been previously reported that hydrido lanthanide complexes supported by guanidinate[16a] and linked cyclopentadienyl- amido[16b] ligands feature monomer-dimer equilibrium due to reversible dissociation in solution. This fact is proved by the formation of heterobimetallic dimers when equimolar amounts of dimeric yttrium and lutetium complexes are mixed in the solution. The ^1H and $^{13}C\{^1H\}$ NMR spectra of the mixture of equimolar amounts of **3Y** and **3Lu** in d^6-benzene (340 h, ambient temperature) present superposition of the spectra of the starting compounds thus giving an evidence for stability of the trinuclear core in solution.

Despite the similarity of the solid state structures of Lu complexes **3Lu** and **2Lu** their hydrido ligands give different sets of signals in the ^1H NMR spectra at 298 K. The ^1H NMR spectrum of **3Lu** displays three singlets (δ = 9.08 (broad), 12.25, 12.37 ppm) with the integral intensities ratio 3:1:1 while for **2Lu** four signals with the chemical shifts 7.71, 11.50, 12.42, 12.51 ppm and the integral intensities ratio 1:1:1:1 are observed. As evidenced by the 2D COSY NMR spectrum of **2Lu** one more signal corresponding to the hydrido ligand overlaps with the aromatic protons signals of amidopyridinato ligands (cross-peaks (7.03;7.71), (7.03;11.50), (7.03;12.42), (7.03;12.51). The number of the signals due to the μ-H ligands in the case of **2Lu** is similar to that reported for the alkyl-hydrido cluster coordinated by bulky cyclopentadienyl ligands $([(C_5Me_4SiMe_3)_2Lu_2(\mu\text{-}H)_5Lu(\mu\text{-}CH_2SiMe_2C_5Me_4)(thf)_2]$[17] 5.54, 6.55, 9.04, 9.13 and 9.68 ppm) however the signals of the hydrido ligands are substantially low field shifted. A low field shift of the signals corresponding to the hydrido ligands at the transition from cyclopentadienyl rare-earth complexes to those coordinated by N-containing ligands proved to be a general pattern.[18] The two low field μ-H signals (at δ = 12.42 and 12.51 ppm) in the NOESY spectrum do not exhibit any cross-peaks while the other hydrido ligands feature intense exchange cross-peaks with each other (see ESI, Fig. SI6). This fact indicates that two hydrido ligands in the Lu_3H_5-core occupy fixed positions at ambient temperature, while three others are involved in a slow in NMR timescale exchange process. Cooling the sample of **3Lu** results in the broadening of the signal at 9.08 ppm (3H) which splits in three signals (7.08, 7.91, and 12.01 ppm) with integral intensity 1:1:1 at the temperatures below 223 K (see ESI, Fig. SI7). The chemical shifts of the lower field hydrido signals (12.25, 12.37 ppm at 293 K) do not undergo substantial changes in the studied temperature range. Thereby at 298 K the hydrido ligands of **3Lu** which appear in the higher field undergo fast in the NMR timescale exchange while for the corresponding hydrido ligands in **2Lu** this exchange is slow.

Using the Eyring equation,[19] and based on the behavior of the resonances of the hydrido ligands undergoing fast exchange the activation parameters at the coalescence temperature were calculated for **3Lu**: $\Delta H^{\#}$ = 12.4±0.4 kcal·mol^{-1} and $\Delta S^{\#}$ = 9.1±1.2 cal·mol^{-1}·K^{-1}. The similar $\Delta H^{\#}$ and $\Delta S^{\#}$ parameters of the hydrido ligand exchange were measured for ruthenium polyhydrido clusters.[20] As it was mentioned above the exchange of hydrido ligands in complex **2Lu** is slow at ambient temperature and noticeable coalescence of the hydrido signals starts at 343 K. The attempt of evaluation of the energetic parameters of the exchange process failed because of rapid decomposition of **2Lu** at that temperature.

It was previously suggested[10a] that in solution similarly to the solid state structure complex **3Y** contains three μ^2- and two μ^3-bridging hydrido ligands. The detailed multinuclear NMR investigation of yttrium alkyl-hydrido cluster **3Y** in solution was undertaken and revealed more complex situation. According to the 2D ^{89}Y-^{1}H HMQC spectrum of **3Y** (see ESI, Fig. SI8) the compound contains three nonequivalent yttrium nuclei bound with hydrido ligands which appear as three signals with chemical shifts 755, 515 and 503 ppm. The 2D ^{89}Y-^{1}H long range correlation spectrum reveals that only one of the yttrium nucleus has spin-spin interactions with CH_2-protons of alkyl group (cross peaks: –1.10;755, –0.03;755 ppm; see ESI, Fig. SI9). The signal corresponding to the yttrium atom covalently bonded to the terminal alkyl group (δ = 755 ppm) is substantially high field shifted compared to two others (δ = 503 and 515 ppm). This fact can be explained both by the coordination of the THF molecules donating electron density to two metal centers (δ = 503 and 515 ppm) and by stronger electron accepting character of the alkyl group (*vs* that of hydrido ligands) bonded to the third one. According to the ^{1}H and 2D ^{89}Y-^{1}H HMQC NMR spectrum **3Y** (see ESI, Fig. SI8) contains two different types of μ-H ligands. Two hydrido ligands which appear as triplets with chemical shifts 7.21 and 7.00 ppm ($^1J_{YH}$ = 32.0 Hz) interact with two yttrium nuclei (cross-peaks (7.21;755), (7.21;515) and (7.00;755), (7.00;503)). These signals should be attributed to the μ^2-bridging hydrido ligands (Figure 6) due to their multiplicity and the observed ^{89}Y-^{1}H interactions. The triplet of doublets at δ = 5.66 ppm in the ^{1}H NMR spectrum should be assigned to three other hydrido ligands. In the ^{89}Y-^{1}H HMQC spectrum these signal displays cross-peaks with all three yttrium atoms of the trinuclear core indicating their μ^3-bridging coordination mode. The multiplicity of this signal (triplet of doublets) originates from strong coupling of hydrido ligands with two Y nuclei ($^1J_{YH}$ = 20.8 Hz) and weaker coupling ($^1J_{YH}$ = 5.8 Hz) with one more Y.

At the ambient temperature three μ^3-H ligands are equivalent in the ^{1}H NMR spectrum, however the variable temperature NMR studies (193–323 K) indicated that **3Y** features a thermally dependent dynamic process. Unfortunately the complexity of the ^{1}H NMR spectra does not allow for determination of the energetic parameters of this process.

Thereby one can conclude that in **3Y** in solution two μ^2-hydrido ligands bridging the yttrium bearing the alkyl group with two THF-solvated yttrium centers are not involved into dynamic process. At the same time the hydride bridging two THF-solvated yttriums exchanges with two μ^3-bridging hydrides located in the apical positions thus also becoming a μ^3-bridging ligand (Fig. 6).

Fig. 6. The exchange scheme for hydrido ligands in alkyl-hydrido complexes.

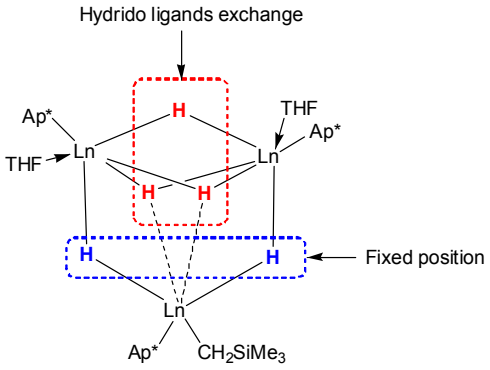

Catalytic activity of alkyl-hydrido complexes

Catalytic activities of previously described trinuclear alkyl-hydrido clusters $[(Ap^*Ln)_3(\mu^2\text{-}H)_3(\mu^3\text{-}H)_2(CH_2SiMe_3)(thf)_2]$ (**3Ln**, Ln = Y, Er, Yb, Lu),[10] cationic yttrium hydrido cluster $[(Ap^*Y)_3(\mu^2\text{-}H)_3(\mu^3\text{-}H)_2(thf)_3]^+[B(C_6F_5)_4]^-$ (**4Y**)[10b] as well as of **2Lu** and **2Yb$^{SiMe3/SiH2Ph}$** were evaluated in ethylene polymerization under mild conditions (toluene, 20 °C, ethylene pressure 0.5 bar). The curves of monomer consumption (mol per mol of catalyst) *vs* time are presented in Fig. 7. For the series of the Ap*-containing alkyl-hydrido complexes catalytic activity predictably turned out dependent on the ionic radius of the metal center. The higher activity was observed for yttrium derivative **3Y** (560 g·mmol^{-1}·bar^{-1}·h^{-1}). The ytterbium (**3Yb**) and lutetium (**3Lu**) containing analogues showed lower activity (165 and 168 g·mmol^{-1}·bar^{-1}·h^{-1} respectively). Unexpectedly the complex of erbium **3Er** having the ionic radius close to that of yttrium (R(Y^{3+}) = 0.960 Å; R(Er^{3+}) = 0.954 Å)[16] performed low activity 12 g·mmol^{-1}·bar^{-1}·h^{-1} and lost the activity in ~1 h. Yttrium cationic polyhydrido derivative **4Y** demonstrated rather high activity (465 g·mmol^{-1}·bar^{-1}·h^{-1}) however induction period of approximately two hours appeared. The passage from Ap*-containing alkyl-hydrido complex **3Yb** to the Ap^{9Me}-derived analogue **2Yb$^{SiMe3/SiH2Ph}$** resulted in the noticeable increase in catalytic activity (165 *vs* 880 g·mmol^{-1}·bar^{-1}·h^{-1}). While the catalytic activity of lutetium complex with Ap^{9Me}-amidopyridinato ligand slightly exceeds that of Ap*-anologue (210 g·mmol^{-1}·bar^{-1}·h^{-1} for **2Lu**; 168 g·mmol^{-1}·bar^{-1}·h^{-1} for **3Lu**).

Alkyl-hydrido and cationic-polyhidrido complexes were inactive in styrene polymerization, but show low activity in polymerization of propylene. Ap*-containing alkyl-hydrido derivatives **3Y** and **3Lu** allowed to produce 64 and 37 g·mmol^{-1}·bar^{-1}·h^{-1} of polypropylene respectively (toluene, 0 °C, propylene pressure 0.5 atm), but both catalysts lost their activity in 5 h. Complexes **3Y** and **4Y** were tested as a single component catalysts for isoprene polymerization. Alkyl-hydrido complex **3Y** was absolutely inactive, while cationic

polyhydride **4Y** demonstrate low activity. At the monomer catalyst ratio 1000/1 after 24 h the isoprene conversion was 45%. The polymer sample demonstrated a bimodal molecular weights distribution. The first polymer fraction has polydispersity index M_w/M_n = 1.57 and molecular weight M_w = $11.6\cdot10^5$, while the second polymer fraction was characterized by polydispersity index M_w/M_n = 1.97 and lower molecular weight M_w = $7.3\cdot10^5$. Complex **4Y** shows moderate selectivity with predominant 1,4-cis-regularity up to 63% (1,4-trans – 4%; 3,4 – 33%).

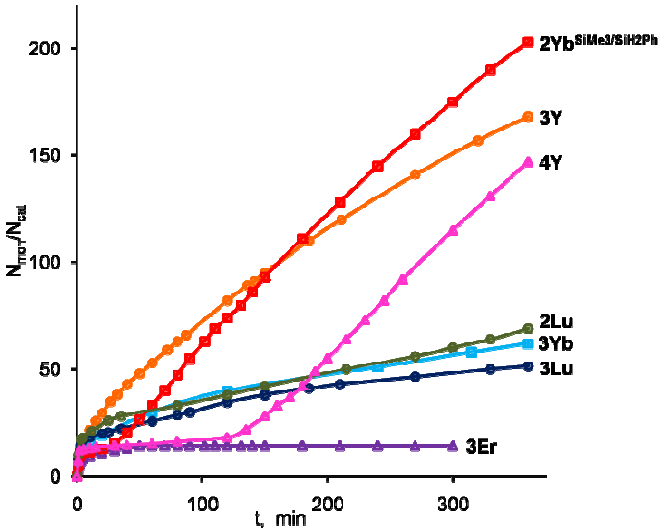

Fig. 7. Plot of ethylene absorption (N_{mon}/N_{cat}) *vs* time (min). — **2Yb$^{SiMe3/SiH2Ph}$**; — **2Lu**; — **4Y**; — **3Y**; — **3Er**; — **3Yb**; — **3Lu**.

Conclusions

The present study demonstrated the role of bulkiness of amidopyridinate ligands in stabilization of trinuclear rare-earth alkyl-hydrido species. The most bulky Ap* ligand allows for stabilization and isolation of alkyl-hydrido clusters $[(Ap^*Ln)_3(\mu^2\text{-}H)_3(\mu^3\text{-}H)_2(CH_2SiMe_3)(thf)_2]$ (Ln = Y, Er, Yb, Lu)[10] of rare earth metals having small (Lu, Yb) and medium (Y, Er) ionic radii. The less bulky Ap^{9Me} turned out suitable for stabilization of analogous structures only for the smallest Lu – $[(Ap^{9Me}Lu)_3(\mu^2\text{-}H)_3(\mu^3\text{-}H)_2(CH_2SiMe_3)(thf)_2]$, while for bigger Y and for having similar size Yb unusual C-Si bond activation reactions occur resulting in the formation of trinuclear alkyl-hydrido species featuring a modified alkyl group $[(Ap^{9Me}Ln)_3(\mu^2\text{-}H)_3(\mu^3\text{-}H)_2(CH_2SiH_2Ph)(thf)_2]$ together with $[(Ap^{9Me}Ln)_3(\mu^2\text{-}H)_3(\mu^3\text{-}H)_2(CH_2SiMe_3)(thf)_2]$ (Ln = Y, Yb). It was found that the $LnCH_2SiH_2Ph$ moiety results from abnormal path of the σ-bond metathesis reaction of bis(alkyl) derivatives $Ap^{9Me}Ln(CH_2SiMe_3)_2(thf)_2$ with $PhSiH_3$. The DFT calculations of $(Ap^*Y)_3(\mu^2\text{-}H)_3(\mu^3\text{-}H)_2(CH_2SiMe_3)(thf)_2$ confirm localization of the HOMO on the Ap*−Y(1A)−CH_2SiMe_3 fragment. Analysis of the electron density distribution reveals the Y−H and H−H bonding interactions in the $(Y)_3(\mu^2\text{-}H)_3(\mu^3\text{-}H)_2$ moiety. The presence of the CH_2SiMe_3 group disturbs the symmetry of the electron density topology and atomic charge distribution in the $(Y)_3(\mu^2\text{-}H)_3(\mu^3\text{-}H)_2$ part of the molecule. According to the ^1H NMR spectra alkyl-hydrido complexes **2Lu** and **3Y**, **3Lu** retain their trinuclear structures in d^6-benzen, d^8-toluene and even in d^8-THF solutions. The detailed multinuclear and variable temperature NMR studies revealed exchange between μ^3- and μ^2-bridging hydrido ligands in **2Lu** and **3Y**, **3Lu** herewith the exchange rate proved to be dependent on the Ap ligand bulkiness. The energetic parameters of hydrido ligand exchange in **3Lu** were measured: $\Delta H^{\#}$ = 12.4±0.4 kcal·mol^{-1} and $\Delta S^{\#}$ = 9.1±1.2 cal·mol^{-1}·K^{-1}. Trinuclear alkyl-hydrido clusters $[(Ap^*Ln)_3(\mu^2\text{-}H)_3(\mu^3\text{-}H)_2(CH_2SiMe_3)(thf)_2]$, cationic yttrium hydrido complex $[(Ap^*Y)_3(\mu^2\text{-}H)_3(\mu^3\text{-}H)_2(thf)_3]^+[B(C_6F_5)_4]^-$ as well as $[(Ap^{9Me}Ln)_3(\mu^2\text{-}H)_3(\mu^3\text{-}H)_2(CH_2SiMe_3)(thf)_2]$ proved to be active in catalysis of ethylene polymerization under mild conditions (toluene, 20 °C, ethylene pressure 0.5 bar). The highest productivities were performed by complex **2Yb^{SiMe3}/Yb^{SiH2Ph}** (880 g·mmol^{-1}·bar^{-1}·h^{-1}) and **3Y** (560 g·mmol^{-1}·bar^{-1}·h^{-1}).

Experimental

All experiments were performed in evacuated tubes, using standard Schlenk-tube or glove-box techniques, with rigorous exclusion of traces of moisture and air. After drying over KOH, THF was purified by distillation from sodium/benzophenone ketyl, hexane and benzene by distillation from sodium/triglyme benzophenone ketyl prior to use. d^6-Benzene, d^8-toluene, d^8-THF were dried with sodium/benzophenone ketyl and condensed in vacuo prior to use. $Ap^{9Me}H$ (2,4,6-trimethylpylphenyl)[6-(2,4,6-triisopropylphenyl)pyridin-2-yl]amine was synthesized according to previously published procedure.[21] Anhydrous $LnCl_3$[22] and $Ln(CH_2SiMe_3)_3(thf)_2$[12] were prepared according to literature procedures. NMR spectra were recorded on a Bruker DPX 200 or Bruker Avance DPX-400 spectrometer. Chemical shifts for ^1H and $^{13}C\{^1H\}$ spectra were referenced internally using the residual solvent resonances and are reported relative to TMS. Chemical shifts for ^{89}Y were externally referenced to YCl_3 in D_2O. Lanthanide metal analysis was carried out by complexonometric titration.[23] The C, H, N elemental analysis was made in the micro analytical laboratory of IOMC.

Synthesis of $Ap^{9Me}Yb(CH_2SiMe_3)_2(thf)$ (1Yb).

A solution of $Ap^{9Me}H$ (0.271 g, 0.65 mmol) in hexane (10 mL) was added to a solution of 0.378 g (0.65 mmol) of $(Me_3SiCH_2)_3Yb(thf)_2$ in hexane (5 mL) at 0 °C. The reaction mixture was stirred for 1 h and then concentrated in vacuum to ¼ of its initial volume. Storing solution at −20 °C overnight resulted in formation of dark red microcrystalline powder of **1Yb**. Mother liqueur was separated by decantation and crystals were dried in vacuum at room temperature for 30 minutes. Compound **1Yb** was isolated in 76% yield (0.413 g, 0.49 mmol). Elemental analysis: Calc. for $C_{41}H_{67}YbN_2OSi_2$: C, 59.10; H, 8.11; N, 3.36; Yb, 20.77. Found: C, 59.23; H, 8.14; N, 3.30; Yb, 20.79.

Synthesis of $Ap^{9Me}Lu(CH_2SiMe_3)_2(thf)$ (1Lu).

The similar synthetic procedure was used. $(Me_3SiCH_2)_3Lu(thf)_2$ (0.295 g, 0.51 mmol) in hexane (5 mL); $Ap^{9Me}H$ (0.210 g, 0.51 mmol) in hexane (10 mL); 0 °C. Compound **1Lu** was isolated as lemon yellow microcrystalline powder in 71% yield (0.305 g, 0.37 mmol). ^{1}H NMR (400 MHz, C_6D_6, 293 K): –0.65 (s, 4H, LuC*H*$_2$), 0.19 (s, 18H, Si(C*H*$_3$)$_3$), 1.17 (d, $^3J_{HH}$ = 6.8 Hz, 6H, C*H*$_3$ C^{25,26,27,28}), 1.22 (br s, 4H, β-C*H*$_2$ THF), 1.32 (d, $^3J_{HH}$ = 6.8 Hz, 6H, C*H*$_3$ C^{29,30}), 1.58 (d, $^3J_{HH}$ = 6.8 Hz, 6H, C*H*$_3$ C^{25,26,27,28}), 2.21 (s, 3H, C*H*$_3$ C^{21}), 2.23 (s, 6H, C*H*$_3$ C^{19,20}), 2.86 (sept, $^3J_{HH}$ = 6.8 Hz, 1H, C*H* C^{24}), 3.11 (sept, $^3J_{HH}$ = 6.8 Hz, 2H, C*H* C^{22,23}), 3.64 (br s, 4H, α-C*H*$_2$ THF), 5.66 (d, $^3J_{HH}$ = 8.6 Hz, 1H, C*H* C^3), 6.17 (d, $^3J_{HH}$ = 7.0 Hz, 1H, C*H* C^5), 6.82 (dd, $^3J_{HH}$ = 8.6 Hz, $^3J_{HH}$ = 7.0 Hz, 1H, C*H* C^4), 6.85 (s, 2H, C*H* C^{15,17}), 7.27 (s, 2H, C*H* C^{9,11}) ppm. ^{13}C{^{1}H} NMR (100 MHz, C_6D_6, 293 K): 4.1 (s, Si(*C*H$_3$)$_3$), 18.7 (s, *C*H$_3$ C^{19,20}), 20.6 (s, *C*H$_3$ C^{21}), 23.1 (s, *C*H$_3$ C^{25,26,27,28}), 24.1 (s, *C*H$_3$ C^{29,30}), 24.8 (s, β-*C*H$_2$ THF), 24.1 (s, *C*H$_3$ C^{25,26,27,28}), 30.6 (s, *C*H C^{22,23}), 34.7 (s, *C*H C^{24}), 46.1 (s, Lu*C*H$_2$), 69.1 (s, α-*C*H$_2$ THF), 104.8 (s, *C*H C^3), 111.2 (s, *C*H C^5), 120.8 (s, *C*H C^{9,11}), 129.1 (s, *C*H C^{15,17}) 132.5 (s, C^{16}), 132.9 (s, C^{14,28}), 135.6 (s, C^7), 139.6 (s, *C*H C^4), 143.9 (s, C^{13}), 145.4 (s, C^{8,12}), 149.3 (s, C^{10}), 155.9 (s, C^6), 166.9 (s, C^2) ppm. Elemental analysis: Calc. for $C_{41}H_{67}LuN_2OSi_2$: C, 58.97; H, 8.09; N, 3.35; Lu, 20.95. Found: C, 59.08; H, 8.17; N, 3.18; Lu, 20.81.

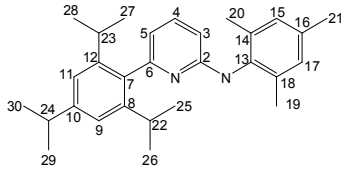

Synthesis of $\{[(Ap^{9Me}Lu)_3(\mu^2\text{-}H)_3(\mu^3\text{-}H)_2(CH_2SiMe_3)(thf)_2]\}$ (2Lu).

Method A) $PhSiH_3$ (0.185 g, 1.70 mmol) was added to solution of $Ap^{9Me}Lu(CH_2SiMe_3)_2(thf)$ (0.706 g, 0.85 mmol) in hexane (20 mL) at 0 °C. The reaction mixture was stirred for 2 h then was slowly warmed up to the ambient temperature and stirred again for 2 h. The reaction mixture was concentrated in vacuum approximately to ¼ of its initial volume and stored at −20 °C overnight. Complex **2Lu** was isolated as yellow crystals in 60% yield (0.341 g, 0.17 mmol). ^{1}H NMR (400 MHz, C_6D_6, 293 K): –0.70 (d, $^2J_{HH}$ = 10.6 Hz, 1H, LuC*H*$_2$), –0.62 (d, $^2J_{HH}$ = 10.6 Hz, 1H, LuC*H*$_2$), 0.42 (s, 9H, Si(C*H*$_3$)$_3$), 1.04–1.35 (complex m, together 56H C*H*$_3$ *i*Pr H^{25,26,27,28,29,30} and β-C*H*$_2$ THF), 1.46 (d, $^3J_{HH}$ = 6.6 Hz, 3H, C*H*$_3$ *i*Pr), 1.68 (d, $^3J_{HH}$ = 6.6 Hz, 3H, C*H*$_3$ *i*Pr), 2.03, 2.14, 2.23, 2.26, 2.27, 2.36, 2.38, 2.59, 2.60 (s, 3H, C*H*$_3$, H^{19,20,21}), 2.70–3.41 (complex m, together 17H C*H* *i*Pr H^{22,23,24} and α-C*H*$_2$ THF), 5.54, 5.57, 5.71 (d, $^3J_{HH}$ = 8.6 Hz, 1H, C*H* H^3), 6.01, 6.03, 6.09 (d, $^3J_{HH}$ = 7.0 Hz, 1H, C*H* H^5), 6.72–7.25 (complex m, together 16H H^{4,9,11,15,17} and Lu(μ-*H*)), 7.71 (s, 1H Lu(μ-*H*)), 11.48 (s, 1H Lu(μ-*H*)), 12.40 (s, 1H Lu(μ-*H*)), 12.49 (s, 1H Lu(μ-*H*)) ppm. ^{13}C{^{1}H} NMR (100 MHz, C_6D_6, 293 K): 5.3 (s, Si(*C*H$_3$)$_3$), 18.7, 19.6, 20.1, 20.4, 20.5, 20.6, 20.7, 20.8, 21.1 (s, *C*H$_3$ C^{19,20,21}), 22.4, 22.7, 23.0, 23.2, 23.6, 23.8, 23.9, 24.0, 24.1, 24.2, 24.4, 24.8, 24.9, 25.2, 25.5, 25.9, 26.0, 26.8, 26.9 (s, *C*H$_3$ C^{25,26,27,28} and β-*C*H$_2$ THF), 30.0, 30.1, 30.2, 30.3, 30.4, 30.5 (s, *C*H C^{22,23}), 34.4, 34.5, 34.6 (s, *C*H C^{21}), 41.8 (s, Lu*C*H$_2$), 69.4, 67.0 (s, α-*C*H$_2$ THF),103.7, 103.8, 105.6 (s, *C*H C^3), 110.6, 110.8, 111.0 (s, *C*H C^5), 120.0, 120.1, 120.3, 120.5, 120.6, 120.8 (s, *C*H C^{9,11}), 128.7, 128.8, 129.1, 129.2, 129.5, 130.0 (s, *C*H C^{15,17}), 130.9, 131.4, 131.5, 132.9, 133.1, 134.4, 134.5, 134.8, 134.9 (s, C^{14,16,18}), 136.4, 136.7, 137.2 (s, C^7), 138.1, 138.8, 139.1 (s, *C*H C^4), 145.3, 145.5, 145.6, 145.9, 146.0, 146.1, 147.3, 147.4, 147.6, 147.7, 148.2, 148.6 (s, C^{8,10,12,13}), 155.5, 155.7, 156.0 (s, C^6), 167.7, 168.4, 170.2 (s, C^2) ppm. Elemental analysis: Calc. for $C_{99}H_{143}Lu_3N_6O_2Si$: C, 59.39; H, 7.20; Lu, 26.22; N, 4.20. Found: C, 59.48; H, 7.44; Lu, 26.08; N 4.13.

Method B) Evacuated 200 mL Shlenck flask equipped with a teflon stop-cock with 20 mL of hexane solution of $Ap^{9Me}Lu(CH_2SiMe_3)_2(thf)$ (0.425 g, 0.51 mmol) was filled with dry H_2 (3 bar). The reaction mixture was stirred for at ambient temperature for 36 h. The reaction mixture was concentrated in vacuum approximately to ¼ of its initial volume and stored at −20 °C overnight. Complex **2Lu** was isolated as yellow crystals in 62% yield (0.221 g, 0.11 mmol).

Synthesis of $\{[(Ap^{9Me}Y)_3(\mu^2\text{-}H)_3(\mu^3\text{-}H)_2(CH_2SiMe_3)(thf)_2]_2[(Ap^{9Me}Y)_3(\mu^2\text{-}H)_3(\mu^3\text{-}H)_2(CH_2SiH_2Ph)(thf)_2]\}$ ($2Y^{SiMe3/SiH2Ph}$)

$PhSiH_3$ (0.177 g, 1.64 mmol) was added to a solution of $Ap^{9Me}Y(CH_2SiMe_3)_2(thf)$ (0.615 g, 0.82 mmol) in hexane (20 mL) at 0 °C. Reaction mixture was stirred for 2 h then was slowly warmed up to the ambient temperature and stirred additionally for 2 h. Reaction mixture was concentrated in vacuum approximately to ¼ of its initial volume and stored at −20 °C for 2 weeks. Yellow crystals of $\mathbf{2Y^{SiMe3/SiH2Ph}}$ were isolated in 7% yield (0.039 g, 0.02 mmol).

Synthesis of $\{[(Ap^{9Me}Yb)_3(\mu^2\text{-}H)_3(\mu^3\text{-}H)_2(CH_2SiMe_3)(thf)_2][(Ap^{9Me}Yb)_3(\mu^2\text{-}H)_3(\mu^3\text{-}H)_2(CH_2SiMe_3)(thf)_2]\}$ ($2Yb^{SiMe3/SiH2Ph}$):

$PhSiH_3$ (0.212 g, 1.96 mmol) was added to a solution of $Ap^{9Me}Yb(CH_2SiMe_3)_2(thf)_2$ (0.816 g, 0.98 mmol) in hexane (20 mL) at 0 °C. Reaction mixture was stirred for 2 h then was slowly warmed up to the ambient temperature and stirred for additional 2 h. The reaction mixture was concentrated in vacuum approximately to ¼ of its initial volume and stored at −20 °C overnight. Red-brownish crystals of $\mathbf{2Yb^{SiMe3/SiH2Ph}}$ were isolated in 64% yield (0.422 g, 0.11 mmol). Elemental analysis: Calc. for $C_{201}H_{284}N_{12}O_4Si_2Yb_6$: C, 59.95; H, 7.11; N, 4.17; Yb, 25.78. Found: C, 60.43; H, 7.52; N, 4.01; Yb 25.43.

DFT

The geometry optimization of $(Ap^*Y)_3(\mu^2\text{-}H)_3(\mu^3\text{-}H)_2(CH_2SiMe_3)$ was carried out at the PBEPBE/DGDZVP[24] level of theory with use of the Gaussian03 package.[25] The calculations involved 4651 primitive gaussians. The absence of imaginary vibrational frequencies was taken as an evidence of a local energy minimum. MO and NBO[26] analyses were performed to investigate the electronic structure and charge distribution in the molecule. The quantum theory "Atoms in Molecules" (QT AIM)[27] was employed to investigate the

electron density topology. The AIMALL program package[28] was used to reveal and analyze the (3,–1) bonding critical points. The RDG function and the λ_2 values were calculated with the Multiwfn 3.2 code.[29]

X-Ray Study

The data for **2Ln** were collected on a SMART APEX diffractometer (graphite-monochromatic, $Mo_{K\alpha}$ radiation, ω- and θ-scan technique, λ = 0.71073 Å). The structures were solved by direct methods and were refined on F^2 using SHELXTL[30] package. All non-hydrogen atoms in **2Ln** were refined anisotropically. Positions of hydride H-atoms were found from fourier synthesis of electron density whereas other hydrogen atoms were placed in calculated positions and were refined in the riding model. SADABS[31] (**2Y$^{SiMe3/SiH2Ph}$**, **2Yb$^{SiMe3/SiH2Ph}$**) and XABS2[32] was used to perform area detector scaling and absorption corrections. CCDC-986618 (**2Y$^{SiMe3/SiH2Ph}$**) and CCDC-986619 (**2Yb$^{SiMe3/SiH2Ph}$**) contain the supplementary crystallographic data for this paper. These data can be obtained free of charge from The Cambridge Crystallographic Data Centre via www.ccdc.cam.ac.uk/data_request/cif.

Acknowledgements

The work was supported by the Russian Science Foundation (Project 14-13-00742).

Notes and references

[a]G. A. Razuvaev Institute of Organometallic Chemistry of Russian Academy of Sciences, 49 Tropinina str., 603950, Nizhny Novgorod, GSP-445, Russia Fax: + 007 831 462 74 97 E-mail: trif@iomc.ras.ru.
[b]A. N. Nesmeyanov Institute of Organoelement Compounds of Russian Academy of Sciences, 28 Vavilova str., 119991, Moscow,GSP-1, Russia
[c]Nizhny Novgorod State University, 23 Gagarin av., 603950, Nizhny Novgorod, Russia.

† Electronic Supplementary Information (ESI) available. See DOI: 10.1039/b000000x/

1 (a) W. J. Evans, J. H. Meadows and A. L. Wayda, *J. Am. Chem. Soc.*, 1982, **104**, 2015; (b) W. J. Evans, J. H. Meadows and T. P. Hanusa, *J. Am. Chem. Soc.*, 1984, **106**, 4454; (c) W. J. Evans, M. S. Sollberger, S. I. Khan and R. Bau, *J. Am. Chem. Soc.*, 1988, **110**, 439; (d) M. Ephritikhine, *Chem. Rev.*, 1997, **97**, 2193.

2 (a) S. N. Ringelberg, A. Meetsma, B. Hessen and J. H. Teuben, *J. Am. Chem. Soc.*, 1999, **121**, 6082; (b) E. L. Werkema, E. Messines, L. Perrin, L. Maron, O. Eisenstein and R. A. Andersen, *J. Am. Chem. Soc.*, 2005, **127**, 7781; (c) L. Maron, E. L. Werkema, L. Perrin, O. Eisenstein and R. A. Andersen, *J. Am. Chem. Soc.*, 2005, **127**, 279; (d) E. L. Werkema, R. A. Andersen, A. Yahia, L. Maron and O. Eisenstein, *Organometallics*, 2009, **28**, 3173.

3 For example, see the following. Hydrogenation: (a) G. Jeske, H. Lauke, H. Mauermann, H. Schumann and T. J. Marks, *J. Am. Chem. Soc.*, 1985, **107**, 8111; (b) V. P. Conticello, L. Brard, M. A. Giardello, Y. Tsyji, M. Sabat, C. L. Stern and T. J. Marks, *J. Am. Chem. Soc.*, 1992, **114**, 2761; (c) E. Abinet, D. Martin, S. Standfuss, H. Kulinna, T. P. Spaniol and J. Okuda, *Chem. Eur. J.*, 2011, **17**, 15014. Polymerization: (d) G. Jeske, H. Lauke, H. Mauermann, P. N. Swepston, H. Schumann and T. J. Marks, *J. Am. Chem. Soc.*, 1985, **107**, 8091; (e) H. Mauermann, P. N. Swepston and T. J. Marks, *Organometallics*, 1985, **4**, 200; (f) G. Jeske, L. E. Schock, P. N. Swepston, H. Schumann and T. J. Marks, *J. Am. Chem. Soc.*, 1985, **107**, 8103; (g) G. Desurmont, Y. Li, H. Yasuda, T. Maruo, N. Kanehisha and Y. Kai, *Organometallics*, 2000, **19**, 1811. Hydrosilylation: (h) G. A. Molander and J. A. C. Romero, *Chem. Rev.*, 2002, **102**, 2161. Silylation of aromatic C-H Bonds: (i) J. Oyamada, M. Nishiura and Zh. Hou, *Angew. Chem. Int. Ed.*, 2011, **50**, 10720. Hydroboration: (j) N. K. Harrison and T. J. Marks, *J. Am. Chem. Soc.*, 1992, **114**, 9220; (k) E. A. Bijpost, R. Duchateau and J. H. Teuben, *J. Mol. Catal.*, 1995, **95**, 121. Carbostannylation: (l) S. D. Wobster, C. J. Stephensos, M. Delferro and T. J. Marka, *Organometallics*, 2013, **32**, 1317.

4 (a) S. Arndt and J. Okuda, *Chem. Rev.*, 2002, **102**, 1593; (b) J. Okuda, *Dalton Trans.*, 2003, 2367.

5 (a) Y. Takenaka and Z. Hou, *Organometallics*, 2009, **28**, 5916; (b) J. Gavenonis and T. Don Tilley, *J. Orgtanomet. Chem.*, 2004, **689**, 870; (c) J. Cheng and Z. Hou, *Chem. Commun.*, 2012, **48**, 814.

6 Selected reviews on metal-hydride complexes of rare-earth elements, see: (a) M. Nishiura and Z. Hou, *Nature Chem.*, 2010, **2**, 257; (b) M. Konkol and J. Okuda, *Coord. Chem. Rev.*, 2008, **252**, 1577; (c) A. A. Trifonov, *Russ. Chem. Rev.*, 2007, **76**, 1051; (d) Z. Hou, M. Nishiura and T. Shima, *Eur. J. Inorg. Chem.*, 2007, 2535; (e) Z. Hou, *Bull. Chem. Soc. Jpn.*, 2003, **76**, 2253; (f) J. Okuda, *Dalton Trans.*, 2003, 2367; (g) S. Arndt and J. Okuda, *Chem. Rev.*, 2002, **102**, 1953.

7 (a) Z. Hou, M. Nishiura and T. Shima, *Eur. J. Inorg. Chem.*, 2007, 2535, and references therein. (b) Z. Hou, Y. Zhang, O. Tardif and Y. Wakatsuki, *J. Am. Chem. Soc.*, 2001, **123**, 9216; (c) D. Cui, O. Tardif and Z. Hou, *J. Am. Chem. Soc.*, 2004, **126**, 1312; (d) Y. Luo, J. Baldamus, O. Tardif and Z. Hou, *Organometallics*, 2005, **24**, 4362; (e) T. Shima and Z. Hou, *J. Am. Chem. Soc.*, 2006, **128**, 8124; (f) X. Li, J. Baldamus, M. Nishiura, O. Tardif and Z. Hou, *Angew. Chem., Int. Ed.*, 2006, **45**, 8184; (g) Y. Luo and Z. Hou, *Organometallics*, 2007, **26**, 2941; (h) M. Yousufuddin, M. J. Gutmann, J. Baldamus, O Tardif, Z. Hou, S. A. Mason, G. J. Mclntyre and R. Bau, *J. Am. Chem. Soc.*, 2008, **130**, 3888; (i) M. Nishiura, J. Baldamus, T. Shima, K. Mori and Z. Hou, *Chem. Eur. J.*, 2011, **17**, 5033; (j) T. Shima, M. Nishiura and Z. Hou, *Organometallics*, 2011, **30**, 2513.

8 (a) M. Ohashi, M. Konkol, I. Del Rosal, R. Poteau, L. Maron and J. Okuda, *J. Am. Chem. Soc.*, 2008, **130**, 6920; (b) P. Cui, T. P. Spaniol and J. Okuda, *Organometallics*, 2013, **32**, 1176; (c) G. M. Ferrence and J. Takats, *J. Organomet. Chem.*, 2002, **647**, 84; (d) J. Cheng, K. Saliu, M. J. Ferguson, R. McDonald and J. Takats, *J. Organomet. Chem.*, 2010, **695**, 2696; (e) J. Cheng, M. J. Ferguson and J. Takats, *J. Am. Chem. Soc.*, 2010, **132**, 2; (f) J. Cheng, T. Shima and Z. Hou, *Angew. Chem. Int. Ed.*, 2011, **50**, 1875.

9 (a) G. M. Ferrence, R. McDonald and J. Takats, *Angew. Chem. Int. Ed.*, 1999, **38**, 2233; (b) C. Ruspic, J. Spielman and S. Harder, *Inorg. Chem.*, 2007, **46**, 5320; (c) I. V. Basalov, D. M. Lyubov, G. K. Fukin, A. S. Shavyrin and A. A. Trifonov, *Angew. Chem. Int. Ed.*, 2012, **51**, 3444; (d) I. V. Basalov, D. M. Lyubov, G. K. Fukin, A. V. Cherkasov and A. A. Trifonov, *Organometallics*, 2013, **32**, 1507.

10 (a) D. Lyubov, C. Döring, G. Fukin, A. Cherkasov, A. Shavyrin, R. Kempe and A. Trifonov, *Organometallics*, 2008, **27**, 2905; (b) D.

Lyubov, C. Döring, S. Ketkov, R. Kempe and A. Trifonov, *Chem. Eur. J.*, 2011, **17**, 3824.

11 W. P. Kretschmer, A. Meetsma, B. Hessen, T. Schmalz, S. Qayyum and R. Kempe, *Chem. Eur. J.*, 2006, **12**, 8969.

12 (a) M. F. Lappert and R. J. Pearce, *J. Chem. Soc., Chem. Commun*., 1973, 126; (b) H. Schumann and J. Müller, *J. Organomet. Chem.*, 1979, **169**, C1.

13 (a) G. G. Skvortsov, G. K. Fukin, A. A. Trifonov, A. Noor, C Doering, and R. Kempe, *Organometallics*, 2007, **26**, 5770; (b) D. M. Lyubov, G. K. Fukin, A. V. Cherkasov, A. S. Shavyrin, A. A. Trifonov, l. Luconi, C. Bianchini, A. Meli and G. Giambastiani, *Organometallics*, 2009, **28**, 1227; (c) L. Luconi, D. M. Lyubov, C. Bianchini, A. Rossin, C. Faggi, G. K. Fukin, A. V. Cherkasov, A. S. Shavyrin, A. A. Trifonov and G. Giambastiani, *Eur. J. Inorg. Chem.*, 2010, 608.

14 R. D. Schannon, Acta Crystallogr., Sect. A: Found. Crystallogr., 1976, **32**, 751.

15 (a) A. D. Becke, *Modern Electronic Structure Theory*; World Scientific: River Edge, NJ, 1995; (b) A. J. Cohen, P. Mori-Sánchez and W. Yang, *Science*, 2008, **321**, 792; (c) E. R. Johnson, S. Keinan, P Mori-Sánchez, J. Contreras-García, A. J. Cohen and W. Yang, *J. Am. Chem. Soc.*, 2010, **132**, 6498.

16 (a) D. M. Lyubov, A. M. Bubnov, G. K. Fukin, F. M. Dolgushin, M. Yu. Antipin, O. Pelcé, M. Schappacher, S. M. Guillaume and A. A. Trifonov, *Eur. J. Inorg. Chem.*, 2008, 2090; (b) S. Arndt, P. Voth, T. P. Spaniol and J. Okuda, *Organometallics*, 2000, **19**, 4690.

17 O. Tardif, M. Nishiura and Z. Hou, *Organometallics*, 2003, **22**, 1171.

18 A. A. Trifonov, G. G. Skvortsov, D. M. Lyubov, N. A. Skorodumova, G. K. Fukin, E. V. Baranov and V. N. Glushakova, *Chem. Eur. J.*, 2006, **12**, 5320 and references therein.

19 (a) G. Binsch and H. Kessler, *Angew. Chem. Int. Ed. Engl.*, 1980, **19**, 411; (b) M. L. H. Green, L. L. Wong and A. Sella, *Organometallics*, 1992, **11**, 2660; (c) P. A. Watson, A. C. Wilis and S. B. Wild, *J. Oragnomet. Chem.*, 1993, **445**, 71.

20 M. Ohashi, K. Matsubara and H. Suzuki, *Organometallics*, 2007, **26**, 2330.

21 N. M. Scott, T. Schareina, O. Tok and R. Kempe, *Eur. J. Inorg. Chem.*, 2004, 3297.

22 M. D. Taylor and C. P. Carter, *J. Inorg. Nucl. Chem.*, 1962, **24**, 387.

23. S. J. Lyle and M. M. Rahman, *Talanta*, 1953, **10**, 1177.

24 (a) J. P. Perdew, K. Burke and M. Ernzerhof, *Phys. Rev. Lett.*, 1996, **77**, 3865; (b) N. Godbout, D. R. Salahub, J. Andzelm and E. Wimmer, *Can. J. Chem.*, 1992, **70**, 560; (c) C. Sosa, J. Andzelm, B. C. Elkin, E. Wimmer, K. D. Dobbs and D. A. Dixon, *J. Phys. Chem.*, 1992, **96**, 6630.

25 M. J. Frisch, G. W. Trucks, H. B. Schlegel, G. E. Scuseria, M. A. Robb, J. R. Cheeseman, J. A. Montgomery, Jr., T. Vreven, K. N. Kudin, J. C. Burant, J. M. Millam, S. S. Iyengar, J. Tomasi, V. Barone, B. Mennucci, M. Cossi, G. Scalmani, N. Rega, G. A. Petersson, H. Nakatsuji, M. Hada, M. Ehara, K. Toyota, R. Fukuda, J. Hasegawa, M. Ishida, T. Nakajima, Y. Honda, O. Kitao, H. Nakai, M. Klene, X. Li, J. E. Knox, H. P. Hratchian, J. B. Cross, C. Adamo, J. Jaramillo, R. Gomperts, R. E. Stratmann, O. Yazyev, A. J. Austin, R. Cammi, C. Pomelli, J. W. Ochterski, P. Y. Ayala, K. Morokuma, G. A. Voth, P. Salvador, J. J. Dannenberg, V. G. Zakrzewski, S. Dapprich, A. D. Daniels, M. C. Strain, O. Farkas, D. K. Malick, A. D. Rabuck, K. Raghavachari, J. B. Foresman, J. V. Ortiz, Q. Cui, A. G. Baboul, S. Clifford, J. Cioslowski, B. B. Stefanov, G. Liu, A. Liashenko, P. Piskorz, I. Komaromi, R. L. Martin, D. J. Fox, T. Keith, M. A. Al-Laham, C. Y. Peng, A. Nanayakkara, M. Challacombe, P. M. W. Gill, B. Johnson, W. Chen, M. W. Wong, C. Gonzalez and J. A. Pople, *Gaussian, Inc.*, Pittsburgh PA, 2003.

26 A. E. Reed, L. A. Curtiss and F. Weinhold, *Chem. Rev.*, 1988, **88**, 899.

27 (a) F. Cortés-Guzmán and R. F. W. Bader, *Coord. Chem. Rev.*, 2005, **249**, 633; (b) R. F. W. Bader, *A Quantum Theory*, Oxford University Press: Oxford, UK, 1990.

28 T. A. Keith, *AIMAll*, version 13.05.06; TK Gristmill Software: Overland Park, KS 2013.

29 (a) T. Lu and F. Chen, *J. Mol. Graph. Model.*, 2012, **38**, 314; (b) T. Lu and F. Chen, *J. Comput. Chem.*, 2012, **33**, 580.

30 G. M. Sheldrick, SHELXTL v.6.12, Structure Determination Software Suite, Bruker AXS, Madison, Wisconsin (USA), 2000.

31 G. M. Sheldrick, SADABS v.2.01, Bruker/Siemens Area Detector Absorption Correction Program, Bruker AXS, Madison, Wisconsin (USA), 1998.

32 S. Parkin, B. Moezzi and H. Hope, *J. Appl. Cryst.*, 1995, **28**, 53.

Trinuclear alkyl-hydrido lutetium cluster $[(Ap^{9Me}Lu)_3(\mu^2\text{-}H)_3(\mu^3\text{-}H)_2(CH_2SiMe_3)(thf)_2]$ supported by amidopyridinate ligand is synthesized. For the Y and Yb analogues C-Si bond activation occurs affording the mixture of $[(Ap^{9Me}Lu)_3(\mu^2\text{-}H)_3(\mu^3\text{-}H)_2(CH_2SiMe_3)(thf)_2]$ and $[(Ap^{9Me}Ln)_3(\mu^2\text{-}H)_3(\mu^3\text{-}H)_2(CH_2SiH_2Ph)(thf)_2]$ (Ln = Y, Yb) clusters.